Translational Oncology
www.transonc.com

Volume 12 Number 8 August 2019 pp. 1045–1055 1045

In Preclinical Model of Ovarian Cancer, the SGK1 Inhibitor SI113 Counteracts the Development of Paclitaxel Resistance and Restores Drug Sensitivity

Lucia D'Antona[*,1], Vincenzo Dattilo[*,1], Giada Catalogna[*], Domenica Scumaci[†], Claudia Vincenza Fiumara[†], Francesca Musumeci[‡], Giuseppe Perrotti[*], Silvia Schenone[‡], Rossana Tallerico[*], Cristina B. Spoleti[*], Nicola Costa[*], Rodolfo Iuliano[*], Giovanni Cuda[†], Rosario Amato[*] and Nicola Perrotti[*]

[*]Department of "Scienze della Salute", University "Magna Graecia" of Catanzaro, Viale Europa, Catanzaro; [†]Department of "Medicina Sperimentale e Clinica", University "Magna Graecia" of Catanzaro, Viale Europa, Catanzaro; [‡]Department of Farmacia, University of Genova, Genova

Abstract

Ovarian cancer is the second most common gynecological malignancy worldwide. Paclitaxel is particularly important in the therapy of ovarian carcinomas, but the treatment efficacy is counteracted by the development of resistance to chemotherapy. The identification of target molecules that can prevent or control the development of chemoresistance might provide important tools for the management of patients affected by ovarian cancer. Serum- and glucocorticoid-regulated kinase 1 (SGK1) appears to be a key determinant of resistance to chemo- and radiotherapy. Specifically, SGK1 affects paclitaxel sensitivity in RKO colon carcinoma cells by modulating the specificity protein 1 (SP1)–dependent expression of Ran-specific GTPase-activating protein (RANBP1), a member of the GTP-binding nuclear protein Ran (RAN) network that is required for the organization and function of the mitotic spindle. SGK1 inhibition might thus be useful for counteracting the development of paclitaxel resistance. Here, we present *in vitro* data obtained using ovarian carcinoma cell lines that indicate that the SGK1 inhibitor SI113 inhibits cancer cell proliferation, potentiates the effects of paclitaxel-based chemotherapy, counteracts the development of paclitaxel resistance, and restores paclitaxel sensitivity in paclitaxel-resistant A2780 ovarian cancer cells. The results were corroborated by preclinical studies of xenografts generated in nude mice through the implantation of paclitaxel-resistant human ovarian cancer cells. The SGK1 inhibitor SI113 synergizes with paclitaxel in the treatment of xenografted ovarian cancer cells. Taken together, these data suggest that SGK1 inhibition should be investigated in clinical trials for the treatment of paclitaxel-resistant ovarian cancer.

Translational Oncology (2019) 12, 1045–1055

Introduction

Ovarian cancer is the second most common gynecological malignancy worldwide, and 75% of cases are diagnosed at an advanced stage.[1] For most patients, multimodal therapy is the internationally accepted standard of care.[2] Paclitaxel is particularly important in the therapy of ovarian carcinomas, but its treatment efficacy is counteracted by the development of resistance to chemotherapy.[3,4] Therefore, the identification of target molecules that can prevent or control the development of chemoresistance might provide important tools for

Address all correspondence to: Perrotti Nicola or Amato Rosario, Department of "Scienze della Salute", University "Magna Graecia" of Catanzaro, Viale Europa, Catanzaro. E-mail: rosario.amato@unicz.it

[1]These authors have contributed equally to this work.

Received 8 April 2019; Revised 8 May 2019; Accepted 9 May 2019

1936-5233/19
https://doi.org/10.1016/j.tranon.2019.05.008

the management of patients affected by ovarian cancer. Multiple signaling pathways have been implicated in resistance to chemotherapy, and innovative therapeutic strategies for overcoming these effects are urgently needed.[5] Recent studies based on array-CGH and gene expression profiles suggest that deregulation of the phosphoinositide 3 kinase / RAC-alpha serine/threonine-protein kinase (PI3K/AKT) pathway is common in ovarian cancer and associated with poorer outcomes,[6] and the loss of phosphatase and tensin homolog (PTEN) or amplification of PI3K or AKT has also been found to be common in these patients.[7] Serum- and glucocorticoid-regulated kinase 1 (SGK1) has recently gained attention in the field of molecular oncology. This ubiquitous protein belongs to the family of serine/threonine kinases that share structural and functional similarities with the AKT family of kinases[8] and is a key enzyme in the hormonal regulation of several ion channels and carriers,[9,10] as well as pumps,[11] enzymes,[12,13] and transcription factors.[14–17] SGK1 is regulated by many factors, including insulin, cyclic adenosine monophosphate (cAMP),[13,18,19] insulin like growth factor-1 (IGF-1),[20] steroids,[21] interleukin-2 (IL-2),[22] and transforming growth factor β (TGFβ),[23] and SGK1 activation requires two progressive phosphorylation steps: the mammalian target of rapamycin (mTOR)–dependent phosphorylation of serine 422 in the hydrophobic motif (H-motif)[24] followed by the PDK1-dependent phosphorylation of threonine 256.[25] Because several pathways involve SGK1, this kinase regulates a wide variety of physiological and pathophysiological functions, including cell proliferation and differentiation,[26] nuclear transport,[27] apoptosis, and inflammation.[22,28] Moreover, recent evidence indicates a correlation between SGK1 expression and events of invasiveness and metastatization.[29–31] A few studies have shown increased SGK1 expression and/or activity in different types of human tumors, including ovarian,[32] multiple myeloma,[33] breast,[34,35] prostate,[36] tongue,[37] endometrial,[38] and non–small cell lung cancer,[39] and other studies have demonstrated that SGK1-knockout mouse models show resistance to chemically induced colon carcinogenesis.[40] Furthermore, SGK1 appears to be a key determinant of resistance to chemo- and radiotherapy.[41–45] Specifically, SGK1 affects Taxol sensitivity in RKO colon carcinoma cells by modulating the SP1-dependent expression of RANBP1, a member of the RAN network that is required for the organization and function of the mitotic spindle. SGK1 silencing induces apoptosis, reduces cell proliferation, and enhances paclitaxel sensitivity in RKO cells, which indicate that it mimics the phenotypic consequences of RANBP1 inactivation,[46] and this phenotype is completely reverted by exogenous RANBP1 expression.[15] Taken together, these data indicate that SGK1 might play a significant role in spindle assembly, genetic instability, and sensitivity to paclitaxel. In different malignant cell lines, such as MCF7 breast carcinoma, A-172 glioma, and RKO colon carcinoma cells, the pharmacological inhibition of SGK1 by SI113 can induce cellular death and thereby reduce the cell number. SI113 rapidly induces apoptosis in RKO colon carcinoma cells, and when used in combination with paclitaxel, the two agents together induce a higher degree of apoptosis than either agent alone, which strongly suggests that SI113 and paclitaxel might be successfully used together.[47] Here, we present *in vitro* data obtained in ovarian carcinoma cell lines and *in vivo* data from ovarian carcinoma xenografts in nude mice that indicate that SI113 inhibits cancer cell proliferation, potentiates the effects of paclitaxel-based chemotherapy, counteracts the development of paclitaxel resistance, and restores sensitivity to paclitaxel in paclitaxel-resistant A2780 ovarian cancer cells.

Results

SI113 and Paclitaxel resistance in A2780 human ovarian cancer cells

Resistance to paclitaxel can be induced in A2780 cells by allowing them to grow in gradually increasing concentrations of paclitaxel. The paclitaxel-sensitive human ovarian cancer cell line A2780 was plated as described in the Methods section ("Development of Paclitaxel Resistance").

The cells were first cultured in the presence of 1 nM paclitaxel (Figure 1*A*), and the cells that developed resistance to 1 nM paclitaxel were used as controls for experiments with paclitaxel 5 nM (Figure 1*B*). The cells that developed resistance to 5 nM paclitaxel were used as controls for experiments with paclitaxel 10 nM (Figure 1*C*). The cells that developed resistance to 10 nM paclitaxel were used as controls for experiments with paclitaxel 20 nM (Figure 1*D*). Briefly, for each paclitaxel concentration, cells resistant to the dose used in the previous experiment were used as controls.

Figure 1, *A* through *D* describes the experimental results obtained with 1, 5, 10,m and 20 nM paclitaxel, respectively, in the absence and presence of SI113 (6 μM). In all the experiments, the combination of both agents was more effective than either agent alone. In Figure 1*A*, A2780 paclitaxel-sensitive cells were used as control cells (**CTRL**). Control cells reached complete confluency and cellular overgrowth (OG) before the 12th day of culture. The proliferation of A2780 paclitaxel-sensitive cells treated with a low dose of paclitaxel (1 nM) did not differ from that of the control cells. The cells treated with SI113 alone reached complete confluency and OG on day 18, whereas the cells treated with the combination of the two agents did not reach complete confluency after 18 days of culture (Figure 1*A*). In Figure 1*B*, A2780 cells resistant to paclitaxel 1 nM, treated with paclitaxel 1 nM, were used as control cells (**CTRL**). Control cells reached complete confluency and cellular OG on the 12th day of culture. Compared with the control cells, treatment with either SI113 (6 μM) or paclitaxel (5 nM) had little effect on cell proliferation and viability, although complete confluency and OG were observed later in the experiment. The concomitant presence of SI113 (6 μM) and paclitaxel (5 nM) induced reductions in cellular viability and proliferation, although the cell number remained notably stable throughout the experiment (Figure 1*B*). In Figure 1*C*, A2780 cells resistant to paclitaxel 5 nM, treated with paclitaxel 5 nM were used as control cells (**CTRL**). Control cells reached complete confluency and OG on day 6, as expected given the cellular chemoresistance. On the other hand, cells resistant to paclitaxel 5 nM, treated with SI113 alone, grew slowly and reached complete confluency and OG only on day 15. This effect is probably attributable to the SI113 molecule itself. Cells resistant to paclitaxel 5 nM grew more slowly in the presence of paclitaxel 10 nM, although the effect was transient since paclitaxel resistance at 10 nM was acquired between 15 and 18 days. The concomitant administration of SI113 (6 μM) and paclitaxel 10 nM resulted in an almost complete annihilation of the tumor cell population (Figure 1*C*). In Figure 1*D*, A2780 cells resistant to paclitaxel 10 nM, treated with paclitaxel 10 nM, were used as control cells (**CTRL**). Again, control cells reached complete confluency and OG on day 6, as expected given the cellular chemoresistance. Cells resistant to paclitaxel 10 nM grew more slowly in the presence of either paclitaxel 20 nM or SI113 (6 μM). The concomitant administration of SI113 (6 μM) and paclitaxel 20 nM resulted again in a complete annihilation of the tumor cell population, suggesting that

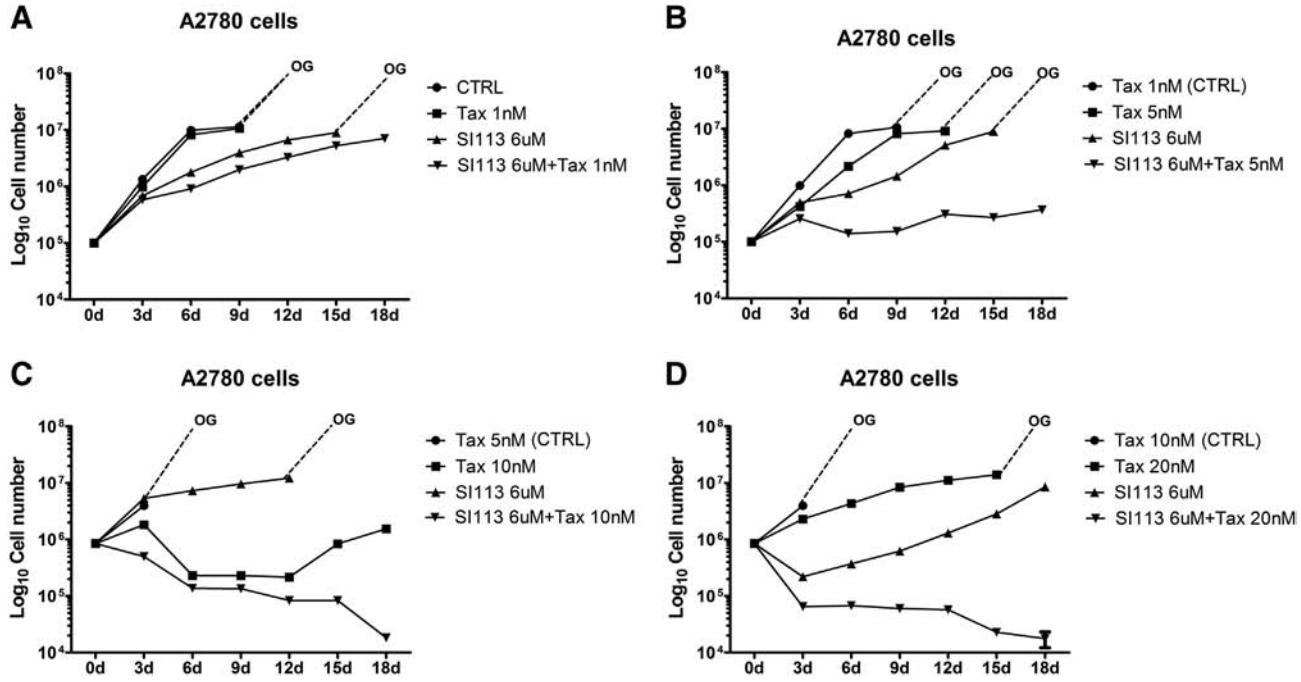

Figure 1. Cell proliferation of A2780 cells based on trypan blue exclusion assays. The inhibition of SGK1 activity by SI113 counteracts the development of paclitaxel resistance in A2780 cells. The experiments were conducted with 1, 5, 10 and 20 nM paclitaxel (A through D, respectively) in the absence and presence of SI113 (6 μM), as indicated. In all the experiments, the combination of both agents is more effective than either agent alone. The effect of SI113 and paclitaxel is very weak at low paclitaxel concentrations (A and B). In contrast, at paclitaxel doses of 10 (C) and 20 nM (D), the concomitant administration of SI113 (6 μM) results in an almost complete annihilation of the tumor cell population, and the development of cells resistant to paclitaxel is inhibited. Statistics are reported in Supplementary Table 1. The results are the averages ± SDs of three independent experiments run in triplicate.

SI113 and paclitaxel exert a strong synergistic effect on the proliferation and survival of A2780 cells (Figure 1*D*). Taken together, the results suggest that the administration of SI113 together with paclitaxel can indeed counteract the development of paclitaxel resistance. Statistically significant differences in cell counting between the different cell culture conditions, as indicated, are reported in Supplementary Table 1**.** When cell counting was not accurate because of the cellular overgrowth, the test was considered not applicable (NA).

SI113 Restores Paclitaxel Sensitivity in Paclitaxel-Resistant Ovarian Cancer Cells

A2780 cells developed paclitaxel resistance through chronic exposures to 100 nM paclitaxel (A2780TC clone[48]), and the resulting A2780TC cells were plated and treated with 100 nM paclitaxel, SI113 at concentrations of 6 μM, 12.5 μM, or both agents together (Figure 2, *A* and *B*). The cells treated with paclitaxel alone showed resistance as expected, whereas the administration of SI113 alone at a dose of 6 μM or 12.5 μM had some effect on cell proliferation. Interestingly, the administration of both agents in combination resulted in a significant inhibition of cell proliferation compared with the effects of either agent alone at the same doses, which confirmed that SI113 treatment sensitizes A2780TC cells to paclitaxel. This effect was even evident in A2780TC cells treated with only 10 nM paclitaxel, which corresponded to 10% of the paclitaxel dose to which the cells showed resistance. Indeed, SI113 treatment at both 6 μM and 12.5 μM restored paclitaxel sensitivity in A2780TC cells, to a paclitaxel dose as low as 10 nM (Figure 2*C*). RNA-specific SGK1 silencing was performed to confirm the involvement of SGK1 in paclitaxel resistance. SGK1 silencing reduced the expression of the kinase by approximately 50% (Supplementary Figure 1). Paclitaxel (10 and 100 nM) significantly reduced the viability of SGK1-silenced A2780TC cells but not control cells (Figure 2*D*), which strongly suggests that SGK1 inhibition might play a role in mediating the effects of SI113 on paclitaxel resistance.

Differential Expression Patterns of Paclitaxel-Sensitive and Paclitaxel-Resistant Human Ovarian Cancer Cell Lines

Sensitivity or resistance to paclitaxel might be characterized by specific expression profiles of candidate genes, such as SGK1 and RANBP1. The differential protein expression patterns related to the development of paclitaxel resistance in A2780 and A2780TC cells were first explored through two-dimensional gel electrophoresis (2DE) followed by a nanoscale liquid chromatography coupled with tandem mass spectrometry (LC–MS/MS) analysis. After automatic spot detection, background subtraction, and volume normalization, 550 spots in A2780TC cells and 491 spots in A2780 cells were detected, and the differences in protein expression were identified based on the relative volume (%Vol, an option of the software that allows an analysis of the data independent of experimental variations between gels caused by differences in loading or staining). The groups were compared through a function interclass analysis, and a fold change of +/−1.8 was considered statistically significant (a report of up- or downregulated proteins is provided in Supplementary Table 2). The results showed that 55 proteins were differentially expressed, and the differentially expressed proteins were analyzed using the

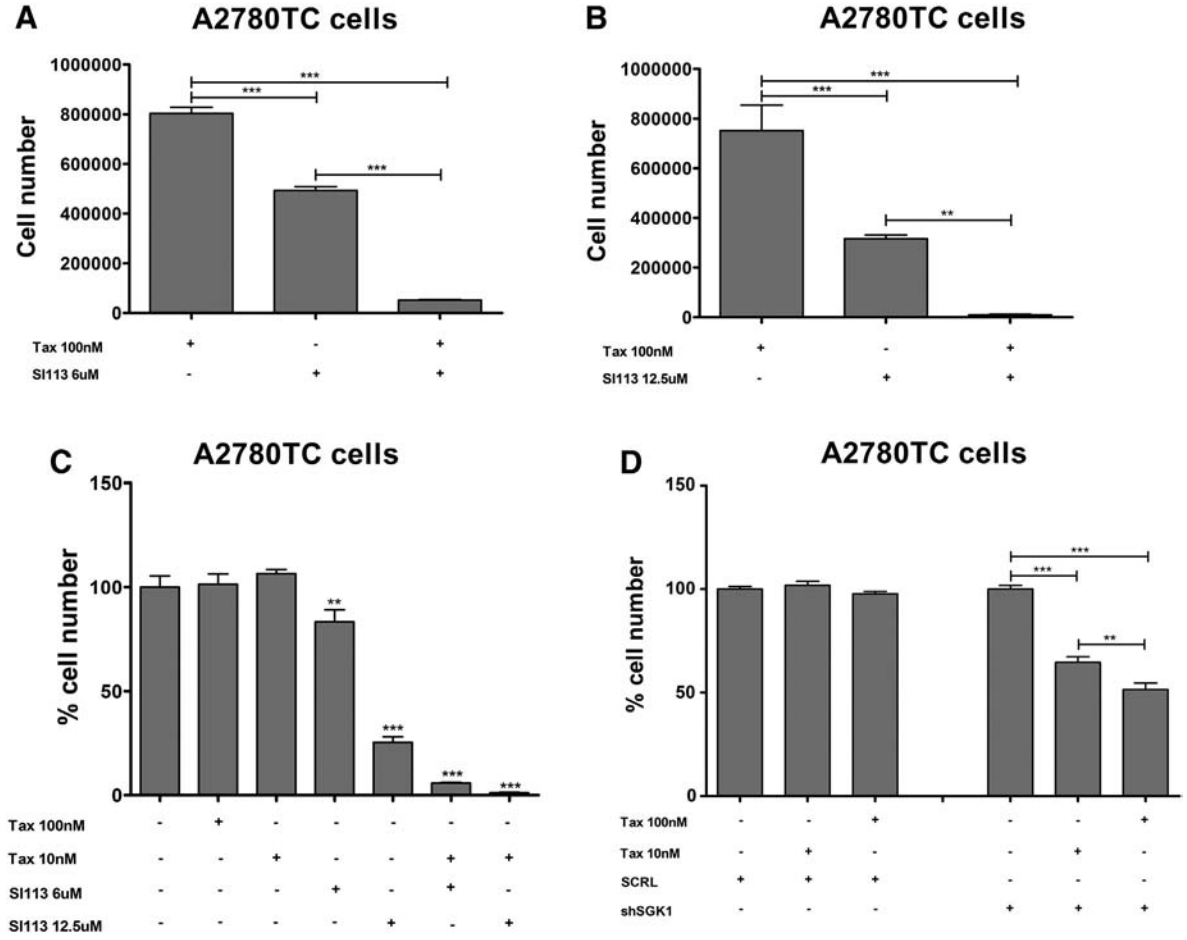

Figure 2. Cell proliferation of A2780TC cells based on trypan blue exclusion assays. The inhibition of SGK1 activity by SI113 restores paclitaxel sensitivity in A2780TC cells. The cells were plated and treated with 100 nM paclitaxel, 6 μM SI113 (A), 12.5 μM SI113 (B), or both agents together. The cells treated with paclitaxel alone show resistance, as expected. SI113 alone at a dose of 6 μM or 12.5 μM has some effect on the cell number, whereas the combination of both agents induces a greater reduction in the cell number compared with that obtained with either agent alone. (C) SI113 treatment at both 6 μM and 12.5 μM restores paclitaxel sensitivity in resistant cells to a dose as low as 10 nM. (D) SGK1 silencing in A2780TC cells restores paclitaxel sensitivity. *$P \leq .05$; **$P \leq .01$; ***$P \leq .001$. The results are presented as the averages ± SDs from three independent experiments run in triplicate.

Ingenuity Pathway Analysis software (IPA) tool (Ingenuity Systems, www.ingenuity.com). Specifically, IPA was used to functionally correlate the differentially expressed proteins with pathways. The software constructs a hypothetical network of protein interactions based on the IPA knowledgebase. Data including the protein IDs and their quantitative expression values were uploaded into the application, and the differentially expressed proteins were overlapped onto global molecular networks generated from information contained in the knowledgebase. Networks were then algorithmically generated based on their connectivity and "named" based on the most common functional group(s) present.[49] The IPA analysis allowed identification of the biological functions that were most significantly associated with the genes in the network. Specifically, the identified proteins were mapped onto five networks, and three of the most representative networks are described in Supplementary Figure 2. The first network, which had a score of 60 and 26 focus molecules, is involved in functions associated with cellular compromise, inflammatory response, and developmental disorder. The second network, which contains 10 focus molecules and was given a score of 17, exhibited functions connected with cell death and survival, developmental disorder, and hereditary disorder. The third network grouped proteins involved in gene expression, developmental disorder, and hereditary disorder (Supplementary Table 3). A biofunctional analysis showed that apoptosis, necrosis, and cell death of tumor cell lines were inhibited in paclitaxel-resistant cells (Supplementary Figure 3). An analysis of the differentially expressed spots between the A2780 and A2780TC cell lines confirmed the presence of Ran-specific GTPase-activating protein [RANG_HUMAN] (RANBP1) (spot 15), coded by the *RANBP1* gene, and GTP-binding nuclear protein Ran [RAN_HUMAN] (spot 5), coded by the *RAN* gene, which were upregulated in A2780TC cells compared to A2780 cells with fold changes of 2.1 and 1.8, respectively (Figure 3*A*). Because our previous studies demonstrated that RANBP1 mediates SGK1-dependent fluctuations in paclitaxel sensitivity,[15] we focused on the differential expression of SGK1 and RANBP1 as genetic markers of paclitaxel resistance. A further analysis showed that the protein expression of SGK1 and RANBP1 was clearly increased in A2780TC compared with A2780 cells (Figure 3*B*). The endogenous mRNA levels of both SGK1 and RANBP1 in sensitive (A2780) and resistant (A2780TC and OVCAR3) human ovarian cancer cell lines

were evaluated by qRT-PCR. The results showed 12-fold and 130-fold increases in SGK1 mRNA levels in A2780TC and OVCAR3 cells, respectively, compared with A2780 cells (Figure 3*C*, left panel), and an increase in the mRNA level of RANBP1 was also found in the resistant cells (Figure 3*C*, right panel). We also evaluated whether paclitaxel (100 nM) treatment could modulate the expression levels of SGK1 and RANBP1 in these cell lines. In A2780 cells, the treatment reduced both the SGK1 and RANBP1 mRNA levels.

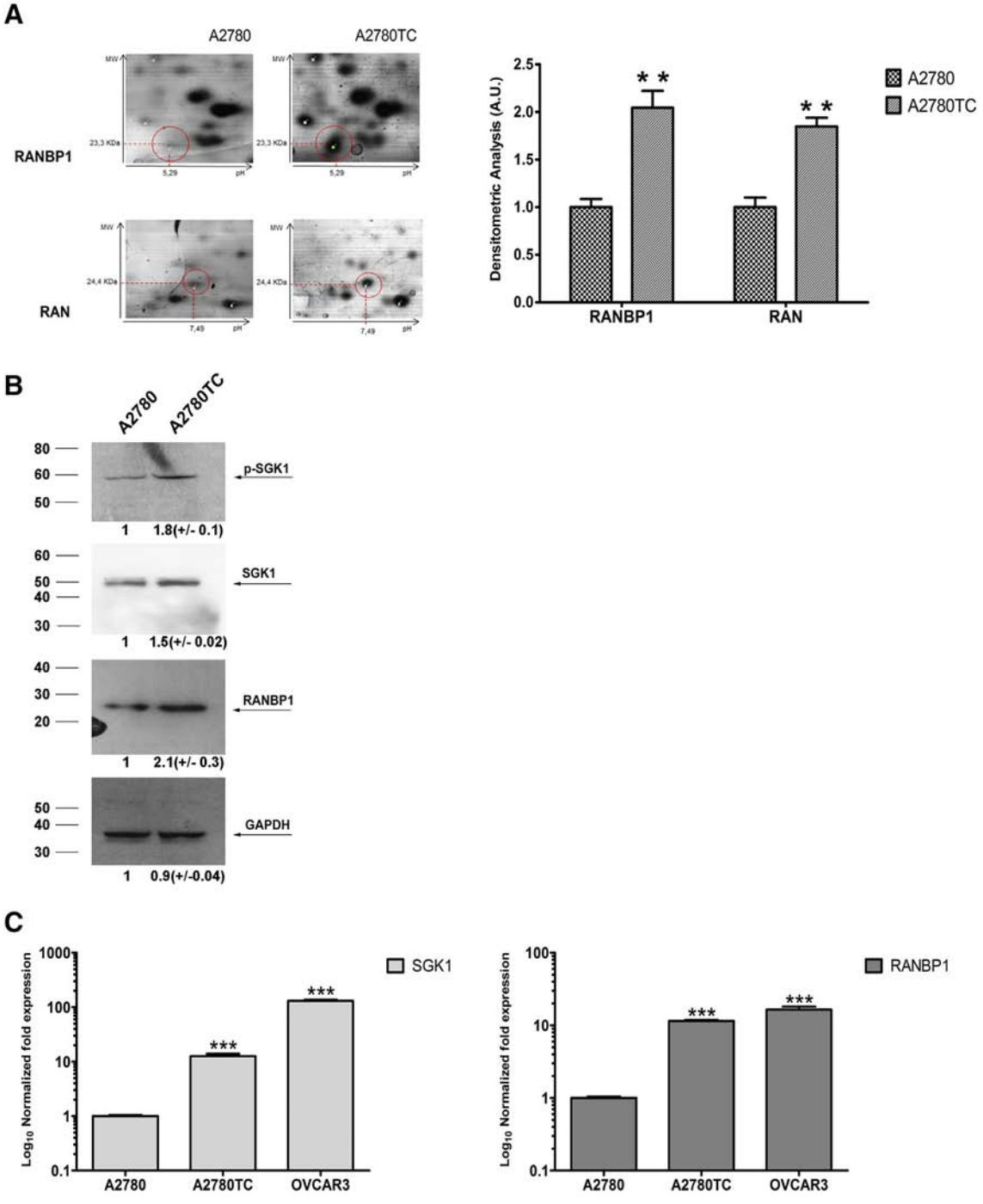

Figure 3. Differential expression patterns between the A2780 and A2780TC cell lines. (A) RANBP1 and RAN spots in 2DE gels from A2780 cells (left) and A2780TC cells (right) and relative densitometric analysis of three independent 2DE gel experiments (right panel). The signal intensity values are expressed as average fold changes ± SDs. (B) Western blot of proteins from A2780 and A2780TC cells. Cell extracts were separated by SDS-PAGE and detected with p-SGK1, SGK1, and RANBP1 antibodies. GAPDH was used as a loading control. The signal intensity values (average fold changes ± SDs) from three independent experiments in both cell lines were obtained by scanning densitometry and are shown under each lane in the blots. (C) qRT-PCR analysis of SGK1 mRNA (left) and RANBP1 mRNA (right) in paclitaxel-sensitive (A2780) and paclitaxel-resistant (A2780TC and OVCAR3) ovarian cancer cell lines. The results, normalized to HPRT1, are presented as the average log10-transformed relative fold expression values ± SDs from triplicate assessments and evaluated by one-way ANOVA. $*P \leq .05$; $**P \leq .01$; $***P \leq .001$.

Conversely, the treatment induced significant increases in the SGK1 and RANBP1 mRNA levels in paclitaxel-resistant cell lines (Figure 4, *A* and *B*). Taken together, these data identify the SGK1 and RANBP1 mRNA expression levels in response to paclitaxel treatment as possible phenotypic hallmarks of paclitaxel sensitivity or resistance. SGK1 enhances the transcription of RANBP1 through the phosphorylation of serine 59 in the N-terminal activation domain of Sp1.[15] We thus wondered whether the RANBP1 expression levels are modulated by the SI113-dependent inhibition of Sgk1 in paclitaxel-sensitive cells (A2780) as well as in resistant cell lines (A2780TC) characterized by enhanced expression of SGK1 and RANBP1. A further analysis showed that A2780 cells were sensitive to the effect of SI113 on the expression of RANBP1: a significant reduction in RNBP1 expression was obtained with SI113 doses as low as 600 nM, and further inhibition was detected at higher doses of the inhibitor (6 μM and 12.5 μM) (Figure 4*C*, left panel). A2780TC cells were resistant to the effect of SI113 on the expression of RANBP1, as demonstrated by a dose–response curve that was clearly shifted toward higher doses of the kinase inhibitor (Figure 4*C*, right panel).

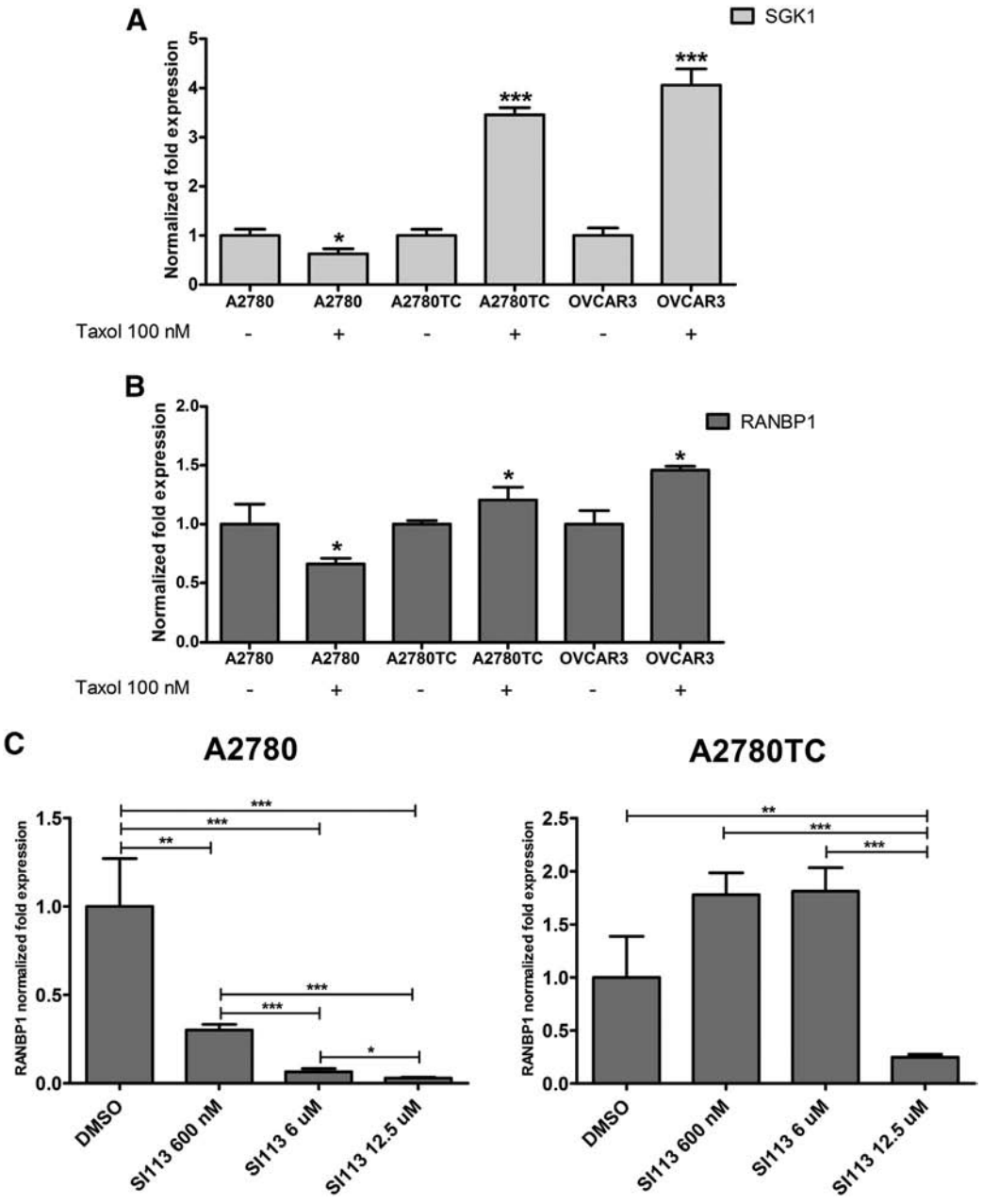

Figure 4. Paclitaxel (100 nM)-dependent modulation of SGK1 (A) and RANBP1 (B) mRNA expression levels (evaluated by qRT-PCR analysis) in paclitaxel-sensitive (A2780) and paclitaxel-resistant (A2780TC and OVCAR3) ovarian cell lines. The results (normalized to the HPRT1 levels) are expressed as the average relative fold expression values ± SDs from triplicate experiments and were evaluated using *t* test. (C) qRT-PCR analysis of RANBP1 mRNA levels in A2780 (left panel) and A2780TC (right panel) after treatment with increasing doses of SI113. The results (normalized to the HPRT1 levels) are expressed as the average relative fold expression values ± SDs from triplicate assessments and were evaluated by one-way ANOVA. *$P \leq .05$; **$P \leq .01$; ***$P \leq .001$.

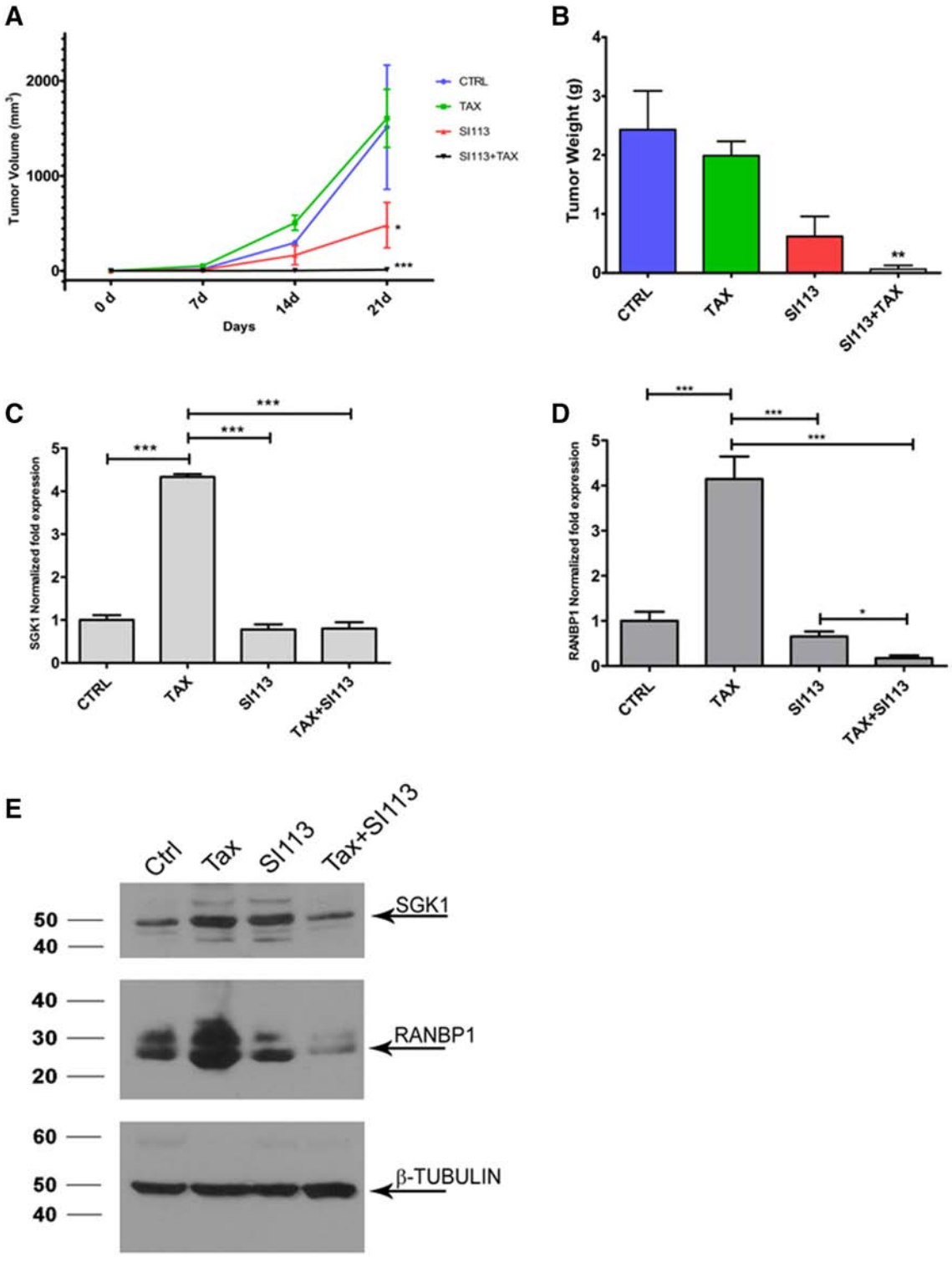

Figure 5. SI113 sensitizes A2780TC xenografts in immunocompromised mice to paclitaxel. (A) Tumor growth curves of animals treated with vehicle alone (control) SI113, paclitaxel, or both agents together. The data are expressed as mm^3 ± standard error (SE) and were evaluated by one-way ANOVA. (B) The mice were sacrificed 21 days after the beginning of the treatment, and their tumors were excised and weighed. The histogram shows the tumor weight (in grams) of each experimental arm expressed in means ± SEs. The differences among the groups were analyzed by one-way ANOVA. (C, D) Quantitative RT-PCR analysis of SGK1 (left) and RANBP1 (right) mRNA levels in tumors from the above-mentioned four experimental arms. The results (normalized to the HPRT1 levels) are expressed as the average relative fold expression values ± SDs from triplicate experiments and were evaluated by one-way ANOVA. (E) Western blot of proteins extracted from A2780TC-derived xenografts treated as indicated. Cell extracts were separated by SDS-PAGE and detected with SGK1 and RANBP1 antibodies. *$P \leq .05$; **$P \leq .01$; ***$P \leq .001$.

SI113 Increases Sensitivity to Paclitaxel Treatment in a Murine Model of Resistant Ovarian Cancer

Based on the *in vitro* studies, we generated xenografts for *in vivo* experiments by implanting 2.5×10^6 paclitaxel-resistant A2780TC cells into the flanks of nude mice. Twenty-four xenografted mice were randomly divided into four experimental groups: i) treatment with the drug vehicle, ii) treatment with paclitaxel (5 mg/kg), iii) treatment with SI113 (9.3 mg/kg), and iv) treatment with the combination of paclitaxel and SI113. The treatments were started 72 hours after cell implantation, and the drugs (or vehicles) were administered 5 days per week. The tumor volumes were measured every 7 days for 21 days, as indicated in the Methods section, and the mice were sacrificed on day 21. The tumors were excised, weighed, and immediately frozen in liquid nitrogen. Paclitaxel treatment had no effect on tumor growth, as expected based on the known chemoresistance of A2780TC cells. The group treated with SI113 showed a significant reduction in tumor volume on day 21 compared with the control group, and a more substantial effect was observed in the mice treated with the combination of paclitaxel and SI113 (Figure 5*A*). The measurements of tumor weight further confirmed the effectiveness of the combination of paclitaxel and SI113 (Figure 5*B*). The excised tumor samples were then processed for detection of the SGK1 and RANBP1 expression levels at both the transcriptional and protein levels through qRT-PC and Western blotting, respectively. The tumors isolated from mice treated with paclitaxel showed increases in the mRNA levels of both SGK1 and RANBP1 compared with the tumors from untreated mice, confirming the results obtained in the A2780TC cells. The administration of SI113 as a single agent had little effect on the expression of SGK1 and RANBP1, whereas a significant reduction in RANBP1 mRNA transcript expression was detected in the tumors from mice treated with both paclitaxel and SI113 compared with those obtained from the control mice (Figure 5, *C* and *D*). All the variations in the transcript levels of SGK1 and RANBP1 obtained between the different experimental groups were confirmed at the protein level (Figure 5*E*).

Discussion

This manuscript describes a continuation and refinement of previous work demonstrating that SGK1 enhances the expression of the gene encoding RANBP1 and induces resistance to paclitaxel in RKO cells. SGK1 silencing increases the sensitivity of cancer cells to paclitaxel, and this effect is counteracted by the ectopic expression of RANBP1. SI113, an SGK1 kinase inhibitor, has been demonstrated to synergize with physical agents (radiotherapy) and drugs (mitotic spindle poisons) to induce apoptotic cell death in several human tumors.

Because the development of paclitaxel resistance is generally considered an important cause of *ovarian cancer* recurrence and is associated with low overall survival,[50] we assessed whether modulation of the SGK1/RANBP1 axis might be helpful for counteracting the development of paclitaxel resistance and restoring sensitivity to the drug in ovarian cancer cell lines. The present study provides the first demonstration that the SGK1 inhibitor SI113 can be helpful for inhibiting the development of paclitaxel resistance in human ovarian cancer cells and can restore paclitaxel sensitivity in cells that are resistant to the drug, and this finding was obtained in cell cultures and in a preclinical mouse model of xenografted human paclitaxel-resistant ovarian cancer. The effect of SI113 was mimicked by SGK1 silencing, which suggested that SGK1 inhibition might play a role in mediating the effects of SI113 on paclitaxel resistance. Through a 2D gel analysis followed by mass spectrometry, we identified several proteins whose expression appears to be related to the development of paclitaxel resistance, and an IPA analysis of differentially expressed proteins identified functional networks related to cellular compromise, inflammatory response, developmental disorder, and cell death and survival. Moreover, our findings demonstrate that the mRNA expression levels of the genes encoding SGK1 and RANBP1 in response to paclitaxel might be considered a hallmark of paclitaxel resistance. In fact, paclitaxel-sensitive and paclitaxel-resistant cells respond to the drug with a significant decrease or increase in the expression of the above-mentioned genes, respectively, which suggests that the hyperexpression of *pro-proliferative* and antiapoptotic *genes might play a role in the development of paclitaxel resistance.* SI113 was originally developed as a dual Src/Abl inhibitor. Given the extensive similarity shared by the ATP-binding sites of several kinases, we cannot confirm the absolute specificity of SI113 for SGK1, although we previously demonstrated that SI113 shows an almost 1000-fold higher selectivity for SGK1 with respect to AKT1[51] and retains some activity toward its original targets.[47] These characteristics show that SI113 is a very interesting kinase inhibitor, and based on the recent identification of SGK1 as a key mediator of Src-induced transformation, a strategy that targets both two kinases could result in enhanced therapeutic efficacy.[52] Because SI113 appears to be well tolerated in mice, we strongly recommend that this molecule be considered for clinical trials involving women with paclitaxel-resistant ovarian cancer.

Materials and Methods

Cell Lines

The paclitaxel-sensitive human ovarian cancer cell line A2780 and the paclitaxel-resistant OVCAR3 cell line were purchased from ATCC (Georgetown University in Washington, DC). Paclitaxel-resistant A2780TC cells were generated by exposing the cells to increasing concentrations of paclitaxel (increased in a stepwise manner) and were cultured in the presence of paclitaxel at a dose of 100 nM to maintain their drug-resistant phenotype (as described by Ferlini et al.[48]).

Development of Paclitaxel Resistance

A2780 cells were plated in 218 wells of six-well plates at a density of 1×10^5 cells: the cells in the 54 control wells were treated with vehicle alone (DMSO), the cells in 54 other wells were treated with paclitaxel (1 nM), the cells in 54 different wells were treated with SI113 (6 μM), and the cells in the remaining 54 wells were treated with both paclitaxel (1 nM) and SI113 (6 μM). The cells were cultured for 18 days, and every 3 days, the cells in three wells from each group were trypsinized and counted by trypan blue exclusion. Fresh tissue culture and treatment medium were added to the remaining wells for continued culture of these cells. The cells that developed resistance to paclitaxel (1 nM) were used for other experiments with progressively higher doses of paclitaxel in the presence and absence of SI113 (6 μM). Specifically, paclitaxel concentrations of 1, 5, 10, and 20 nM were used, and at each paclitaxel concentration, cells resistant to the previous dose of paclitaxel were used as controls.

Cell Viability Assay

Cell proliferation was evaluated by measuring the total number of cells using a Bürker chamber. A2780TC cells, SGK1-silenced cells,

and SCRL A2780TC cells were seeded at a density of 3×10^5 cells/ml in six-well plates. The cell viability, which was determined using a trypan blue exclusion dye, is expressed either as the cell number or percentage of vehicle-treated controls, as indicated.

Lentiviral Production and Cell Transduction

pLKO.1-puro-shSGK1 (Sigma 08041814MN, TCR0000040175) for the RNA interference experiments and shSCRL (Sigma SHC002V) as a control were prepared as previously described[41] and used to generate lentiviral particles in HEK293T packaging cells. Supernatants from shSGK1- or shSCRL HEK293T cells were collected and used for the transduction of A2780TC cells in the presence of 8 μg/ml polybrene (Sigma).

2D PAGE

A2780 and A2780TC cells were washed twice with 1× PBS and, after the PBS was carefully removed, 500 μl of lysis buffer containing 15 mM Tris HCl pH 7.5, 120 mM sodium chloride, 30 mM potassium chloride, 0.1% dithiothreitol (DTT), and 05% Triton X-100 supplemented with protease and phosphatase inhibitor cocktail (Halt Protease Inhibitor Cocktail/Halt Phosphatase Inhibitor Cocktail, Thermo Fisher Scientific Inc). The cells were then scraped, and the resulting cell suspension was collected, incubated at 0°C for 30 minutes, and sonicated using Ultrasonic Baths (VWR) at 4°C for 10 seconds. The cell lysate was centrifuged at 15,000 ×*g* for 20 minutes. The supernatant was carefully removed, and the protein content was measured using the Bradford method (Bio-Rad, Hercules, CA) according to the manufacturer's instructions. The supernatants were stored at 80°C. A total of 120 μg of protein was diluted into isoelectrofocusing (IEF) sample buffer containing 8 M urea, 4% CHAPS, 0.1 M DTT, and 0.8% pH 3-10 nonlinear (NL) carrier ampholyte buffer. IEF was performed on nonlinear immobilized pH gradients (pH 3-10 NL; 24-cm-long IPG strips; GE Healthcare). The first-dimension IPG strips were run on a GE Healthcare IPGphor unit until a total of 50,000 Vh was reached. Prior to SDS-PAGE, the IPG strips were equilibrated with a dithiothreitol (10 mg/ml) SDS equilibration solution followed by treatment with iodoacetamide (25 mg/ml) SDS equilibration solution as described in the GE Healthcare Ettan DIGE protocol. The second-dimension separation was performed using 10% SDS–polyacrylamide gels (2 W/gel; 25°C) until the bromophenol blue dye front reached the end of the gels.[53] The gels were stained with MS-compatible silver staining procedure.[54] The protein spots were analyzed in terms of volume using Image Master 2D-Platinum software, version 6.0 (GE Healthcare BioSciences).[53–55] The protein spots showing a differential expression profile were manually excised from the silver-stained gel using OneTouch Plus Spotpicker (Gel company), destained, and in-gel digested as previously reported.[56–58] The resulting tryptic peptides were purified using Pierce C18 Spin Columns (Thermo Fisher Scientific Inc.) according to the manufacturer's recommended procedure, eluted with 40 μl of 70% acetonitrile, and dehydrated in a vacuum evaporator.[23]

Nanoscale LC–MS/MS Analysis

Tryptic peptides were analyzed using Nanoscale LC–MS/MS[50]. The LC–MS/MS analysis was performed using an Easy LC 1000 nanoscale liquid chromatography (nanoLC) system (Thermo Fisher Scientific, Odense, Denmark). The analytical nanoLC column was a pulled fused silica capillary (75-μm i.d.) that was packed in house to a length of 10 cm with 3-μm C18 silica particles from Dr. Maisch (Entringen, Germany). The purified peptides were resuspended using 0.1% formic acid and loaded at 500 nl/min on the analytical column. The peptides were eluted using a binary gradient. Mobile phase A consisted of 0.1% formic acid and 2% acetonitrile, whereas mobile phase B was 0.1% formic acid and 80% acetonitrile. Gradient elution was performed at a flow rate of 350 nl/min using the following program: 0% B to 30% B in 15 minutes, 30% B to 100% B in 5 minutes, and 100% for 5 minutes. The column was reequilibrated with 0% B for 10 minutes before the following injection. MS detection was performed using a Q Exactive quadrupole-orbitrap mass spectrometer (Thermo Fisher Scientific, Bremen, Germany) operated in the positive ion mode and with nanoelectrospray (nESI) potential of 1800 V applied at the column front-end *via* a tee-piece. Data-dependent acquisition was performed using a top-5 method with the following parameters for full MS and MS/MS: resolution (FWHM), 70,000/17,500; AGC target, 1e6/5e5; and maximum injection time (milliseconds), 50/400. The mass window for precursor ion isolation was 2.0 *m/z*, whereas the normalized collision energy was 30. The ion threshold for triggering MS/MS events was 2e4, and dynamic exclusion was 15 seconds. Proteome Discoverer 1.3 was used for data processing (Thermo Fisher Scientific, Bremen, Germany) using Sequest as the search engine and the HUMAN-refprot-isoforms.fasta as the sequence database. The following search parameters were used: MS tolerance, 15 ppm; MS/MS tolerance, 0.02 Da; fixed modifications, carbamidomethylation of cysteine; variable modification, oxidation of methionine, phosphorylation of serine, threonine and tyrosine; enzyme, trypsin; max. missed cleavages, 2; and taxonomy, human. We consider only those protein hits based on two successful peptide identifications (Xcorr>2.0 for doubly charged peptides, >2.5 for triply charged peptides, and> 3.0 for peptides with a charge state >3) as valid.

Immunoblotting and Immunoprecipitation

The cells were processed as indicated previously[15] and probed with a goat polyclonal RANBP1 antibody (sc-1160, Santa Cruz Biotechnology, Santa Cruz, CA), a rabbit polyclonal SGK1 antibody (cat# 07-315, EDM Millipore Corporation, CA), a rabbit monoclonal p-SGK1 (Ser78) antibody (#D36D11, Cell Signaling, Danvers, MA), a rabbit polyclonal GAPDH antibody (sc-25778, Santa Cruz Biotechnology), and β-tubulin antibody (cat# MA5-16308, Thermo Fischer, Waltham, MA).

Quantitative Real-Time PCR

RNA extraction was performed using the miRNeasy Mini Kit (Qiagen, Valencia, CA) following the manufacturer's instructions. RNA was quantified using a Multiskan Go spectrophotometer (Thermo Scientific, Waltham, MA). The quality of RNA was assayed by determining the 260/280 absorbance ratio and through formaldehyde agarose gel electrophoresis. One microgram of total RNA was subjected to reverse transcription using the High-Capacity RNA-to-cDNA Kit (Applied Biosystems, Foster City, CA) according to the manufacturer's instructions. One microliter of cDNA was amplified *via* real-time PCR using Promega SYBR green (Promega, Madison, WI) and 10 pmol of specific primers.[27,59] The relative expression levels of mRNAs were calculated with the comparative $2^{-\Delta\Delta Ct}$ method using HPRT1 as the housekeeping gene. The real-time PCR assays were performed in triplicate in a total volume of 20 μl using a Bio-Rad iQ 5 apparatus under the following conditions: initial denaturation step of 95°C for 3 minutes followed by 40 cycles of 10 seconds at 95°C and 1 minute at 57°C. The specificity of the PCR products was determined through melting curve analysis.

Mice Treatment

For the *in vivo* experiments, paclitaxel was used at a concentration of 10 mg/kg/day, and SI113 (50 mM in DMSO) was diluted 1:5 in saline solution to obtain a final concentration of 10 mM. Forty-three microliters of the solution was injected intraperitoneally into xenografted nude female mice to obtain a final *in vivo* concentration of approximately 12.5 μM, which corresponds to a dose of 9.3 mg/kg/day assuming a drug distribution volume in the animal of 35 ml. The female nude mice (aged 4 weeks, Charles River) were maintained under pathogen-free conditions and given food/water *ad libitum*. The experiments were performed in accordance with the Catanzaro University Institutional Animal Care and Use Committee guidelines using an approved protocol. At 6 weeks of age, the mice were subcutaneously injected with 2.5×10^6 A2780TC cells suspended in 200 μl of a 1:1 solution containing RPMI without serum and Matrigel solution (BD Collaborative Research) in the dorsal posterior-lateral right region. The mice were randomly assigned to four groups of six animals and then administered vehicle alone (DMSO), SI113, paclitaxel, or both agents for 5 days/week. The tumor volumes were measured every 7 days using caliper. Specifically, two perpendicular diameters (a = smaller diameter; b = larger diameter) were measured, and the tumor volume was calculated in accordance with the formula $V = \pi/6 \times a^2 \times b$. The mice were placed under general anesthesia and sacrificed by vertebral dislocation.

Statistical Analysis

All the tests were performed at least in triplicate, and all the experiments were performed at least three times. The results are expressed as the means ± standard deviations (SDs). The differences between groups were analyzed using Student's t test or one-way analysis of variance (ANOVA) followed by Bonferroni's test for multiple comparisons. The analysis was conducted using GraphPad Prism software (San Diego, CA), and differences were considered significant at $^*P \le .05$, $^{**}P \le .01$, and $^{***}P \le .001$.

Ethical statement

The experimental protocols were approved by the Research Committee of the Department of Health Sciences (University "Magna Graecia" of Catanzaro). The animal experiments were performed in accordance with the Catanzaro University Institutional Animal Care and Use Committee guidelines using an approved protocol.

Supplementary data to this article can be found online at https://doi.org/10.1016/j.tranon.2019.05.008.

Declaration of Competing Interest

The authors declare that they have no conflict of interest.

Acknowledgements

This work was supported by Associazione Italiana per la Ricerca sul Cancro (AIRC; project code IG-16971) and by PON-MIUR 03PE000_78 NUTRAMED. Vincenzo Dattilo was supported by the AIRC 1-year fellowship "CONAD" (Rif. 20946).

References

[1] Ferlay J, Soerjomataram I, Dikshit R, Eser S, Mathers C, and Rebelo M, et al (2015). Cancer incidence and mortality worldwide: sources, methods and major patterns in GLOBOCAN 2012. *Int J Cancer* **136**, E359-386.

[2] Maringe C, Walters S, Butler J, Coleman MP, Hacker N, and Hanna L, et al (2012). Stage at diagnosis and ovarian cancer survival: evidence from the International Cancer Benchmarking Partnership. *Gynecol Oncol* **127**, 75–82.

[3] Bani MR, Nicoletti MI, Alkharouf NW, Ghilardi C, Petersen D, and Erba E, et al (2004). Gene expression correlating with response to paclitaxel in ovarian carcinoma xenografts. *Mol Cancer Ther* **3**, 111–121.

[4] Eisenhauer EA (2017). Real-world evidence in the treatment of ovarian cancer. *Ann Oncol* **28**, viii61–viii65.

[5] Norouzi-Barough L, Sarookhani MR, Sharifi M, Moghbelinejad S, Jangjoo S, and Salehi R (2018). Molecular mechanisms of drug resistance in ovarian cancer. *J Cell Physiol* **233**, 4546–4562.

[6] Huang J, Zhang L, Greshock J, Colligon TA, Wang Y, and Ward R, et al (2011). Frequent genetic abnormalities of the PI3K/AKT pathway in primary ovarian cancer predict patient outcome. *Genes Chromosomes Cancer* **50**, 606–618.

[7] Kuo K-T, Mao T-L, Jones S, Veras E, Ayhan A, and Wang T-L, et al (2009). Frequent activating mutations of PIK3CA in ovarian clear cell carcinoma. *Am J Pathol* **174**, 1597–1601.

[8] Bruhn MA, Pearson RB, Hannan RD, and Sheppard KE (2010). Second AKT: the rise of SGK in cancer signalling. *Growth Factors* **28**, 394–408.

[9] Faletti CJ, Perrotti N, Taylor SI, and Blazer-Yost BL (2002). sgk: an essential convergence point for peptide and steroid hormone regulation of ENaC-mediated Na+ transport. *Am J Physiol Cell Physiol* **282**, C494–C500.

[10] Lang F, Böhmer C, Palmada M, Seebohm G, Strutz-Seebohm N, and Vallon V (2006). (Patho)physiological significance of the serum- and glucocorticoid-inducible kinase isoforms. *Physiol Rev* **86**, 1151–1178.

[11] Wulff P, Vallon V, Huang DY, Völkl H, Yu F, and Richter K, et al (2002). Impaired renal Na(+) retention in the sgk1-knockout mouse. *J Clin Invest* **110**, 1263–1268.

[12] Menniti M, Iuliano R, Föller M, Sopjani M, Alesutan I, and Mariggiò S, et al (2010). 60kDa lysophospholipase, a new Sgk1 molecular partner involved in the regulation of ENaC. *Cell Physiol Biochem* **26**, 587–596.

[13] Menniti M, Iuliano R, Amato R, Boito R, Corea M, and Le Pera I, et al (2005). Serum and glucocorticoid-regulated kinase Sgk1 inhibits insulin-dependent activation of phosphomannomutase 2 in transfected COS-7 cells. *Am J Physiol Cell Physiol* **288**, C148–C155.

[14] Sahin P, McCaig C, Jeevahan J, Murray JT, and Hainsworth AH (2013). The cell survival kinase SGK1 and its targets FOXO3a and NDRG1 in aged human brain. *Neuropathol Appl Neurobiol* **39**, 623–633.

[15] Amato R, Scumaci D, D'Antona L, Iuliano R, Menniti M, and Di Sanzo M, et al (2013). Sgk1 enhances RANBP1 transcript levels and decreases taxol sensitivity in RKO colon carcinoma cells. *Oncogene* **32**, 4572–4578.

[16] Tai DJC, Su C-C, Ma Y-L, and Lee EHY (2009). SGK1 phosphorylation of IkappaB Kinase alpha and p300 Up-regulates NF-kappaB activity and increases N-Methyl-D-aspartate receptor NR2A and NR2B expression. *J Biol Chem* **284**, 4073–4089.

[17] Wang X, Bhattacharyya D, Dennewitz MB, Kalinichenko VV, Zhou Y, and Lepe R, et al (2003). Rapid hepatocyte nuclear translocation of the Forkhead Box M1B (FoxM1B) transcription factor caused a transient increase in size of regenerating transgenic hepatocytes. *Gene Expr* **11**, 149–162.

[18] Perrotti N, He RA, Phillips SA, Haft CR, and Taylor SI (2001). Activation of serum- and glucocorticoid-induced protein kinase (Sgk) by cyclic AMP and insulin. *J Biol Chem* **276**, 9406–9412.

[19] Boito R, Menniti M, Amato R, Palmieri C, Marinaro C, and Iuliano R, et al (2005). RFX-1, a putative alpha Adducin interacting protein in a human kidney library. *FEBS Lett* **579**, 6439–6443.

[20] Boini KM, Bhandaru M, Mack A, and Lang F (2008). Steroid hormone release as well as renal water and electrolyte excretion of mice expressing PKB/SGK-resistant GSK3. *Pflugers Arch* **456**, 1207–1216.

[21] Chen SY, Bhargava A, Mastroberardino L, Meijer OC, Wang J, and Buse P, et al (1999). Epithelial sodium channel regulated by aldosterone-induced protein sgk. *Proc Natl Acad Sci U S A* **96**, 2514–2519.

[22] Amato R, Menniti M, Agosti V, Boito R, Costa N, and Bond HM, et al (2007). IL-2 signals through Sgk1 and inhibits proliferation and apoptosis in kidney cancer cells. *J Mol Med (Berl)* **85**, 707–721.

[23] Lang F and Voelkl J (2013). Therapeutic potential of serum and glucocorticoid inducible kinase inhibition. *Expert Opin Investig Drugs* **22**, 701–714.

[24] García-Martínez JM and Alessi DR (2008). mTOR complex 2 (mTORC2) controls hydrophobic motif phosphorylation and activation of serum- and glucocorticoid-induced protein kinase 1 (SGK1). *Biochem J* **416**, 375–385.

[25] Hong F, Larrea MD, Doughty C, Kwiatkowski DJ, Squillace R, and Slingerland JM (2008). mTOR-raptor binds and activates SGK1 to regulate p27 phosphorylation. *Mol Cell* **30**, 701–711.

[26] Amato R, D'Antona L, Porciatti G, Agosti V, Menniti M, and Rinaldo C, et al (2009). Sgk1 activates MDM2-dependent p53 degradation and affects cell proliferation, survival, and differentiation. *J Mol Med (Berl)* **87**, 1221–1239.

[27] Dattilo V, D'Antona L, Talarico C, Capula M, Catalogna G, and Iuliano R, et al (2017). SGK1 affects RAN/RANBP1/RANGAP1 via SP1 to play a critical role in pre-miRNA nuclear export: a new route of epigenomic regulation. *Sci Rep* **7**, 45361.

[28] Spagnuolo R, Dattilo V, D'Antona L, Cosco C, Tallerico R, and Ventura V, et al (2018). Deregulation of SGK1 in ulcerative colitis: a paradoxical relationship between immune cells and colonic epithelial cells. *Inflamm Bowel Dis* **24**, 1967–1977.

[29] Xiaobo Y, Qiang L, Xiong Q, Zheng R, Jianhua Z, and Zhifeng L, et al (2016). Serum and glucocorticoid kinase 1 promoted the growth and migration of non-small cell lung cancer cells. *Gene* **576**, 339–346.

[30] Huang A-H, Pan S-H, Chang W-H, Hong Q-S, Chen JJW, and Yu S-L (2015). PARVA promotes metastasis by modulating ILK signalling pathway in lung adenocarcinoma. *PLoS One* **10**e0118530.

[31] Davidson B, Abeler VM, Førsund M, Holth A, Yang Y, and Kobayashi Y, et al (2014). Gene expression signatures of primary and metastatic uterine leiomyosarcoma. *Hum Pathol* **45**, 691–700.

[32] Stringer-Reasor EM, Baker GM, Skor MN, Kocherginsky M, Lengyel E, and Fleming GF, et al (2015). Glucocorticoid receptor activation inhibits chemotherapy-induced cell death in high-grade serous ovarian carcinoma. *Gynecol Oncol* **138**, 656–662.

[33] Fagerli U-M, Ullrich K, Stühmer T, Holien T, Köchert K, and Holt RU, et al (2011). Serum/glucocorticoid-regulated kinase 1 (SGK1) is a prominent target gene of the transcriptional response to cytokines in multiple myeloma and supports the growth of myeloma cells. *Oncogene* **30**, 3198–3206.

[34] Sommer EM, Dry H, Cross D, Guichard S, Davies BR, and Alessi DR (2013). Elevated SGK1 predicts resistance of breast cancer cells to Akt inhibitors. *Biochem J* **452**, 499–508.

[35] Hall BA, Kim TY, Skor MN, and Conzen SD (2012). Serum and glucocorticoid-regulated kinase 1 (SGK1) activation in breast cancer: requirement for mTORC1 activity associates with ER-alpha expression. *Breast Cancer Res Treat* **135**, 469–479.

[36] Isikbay M, Otto K, Kregel S, Kach J, Cai Y, and Vander Griend DJ, et al (2014). Glucocorticoid receptor activity contributes to resistance to androgen-targeted therapy in prostate cancer. *Horm Cancer* **5**, 72–89.

[37] Zheng G, Jia X, Peng C, Deng Y, Yin J, and Zhang Z, et al (2015). The miR-491-3p/mTORC2/FOXO1 regulatory loop modulates chemo-sensitivity in human tongue cancer. *Oncotarget* **6**, 6931–6943.

[38] Conza D, Mirra P, Calì G, Tortora T, Insabato L, and Fiory F, et al (2017). The SGK1 inhibitor SI113 induces autophagy, apoptosis, and endoplasmic reticulum stress in endometrial cancer cells. *J Cell Physiol* . http://dx.doi.org/10.1002/jcp.25850.

[39] Abbruzzese C, Mattarocci S, Pizzuti L, Mileo AM, Visca P, and Antoniani B, et al (2012). Determination of SGK1 mRNA in non-small cell lung cancer samples underlines high expression in squamous cell carcinomas. *J Exp Clin Cancer Res* **31**, 4.

[40] Nasir O, Wang K, Föller M, Gu S, Bhandaru M, and Ackermann TF, et al (2009). Relative resistance of SGK1 knockout mice against chemical carcinogenesis. *IUBMB Life* **61**, 768–776.

[41] Talarico C, D'Antona L, Scumaci D, Barone A, Gigliotti F, and Fiumara CV, et al (2015). Preclinical model in HCC: The SGK1 kinase inhibitor SI113 blocks tumor progression in vitro and in vivo and synergizes with radiotherapy. *Oncotarget* **6**. http://dx.doi.org/10.18632/oncotarget.5527.

[42] Talarico C, Dattilo V, D'Antona L, Barone A, Amodio N, and Belviso S, et al (2016). SI113, a SGK1 inhibitor, potentiates the effects of radiotherapy, modulates the response to oxidative stress and induces cytotoxic autophagy in human glioblastoma multiforme cells. *Oncotarget* . http://dx.doi.org/10.18632/oncotarget.7520.

[43] Talarico C, Dattilo V, D'Antona L, Menniti M, Bianco C, and Ortuso F, et al (2016). SGK1, the new player in the game of resistance: chemo-radio molecular target and strategy for inhibition. *Cell Physiol Biochem* **39**, 1863–1876.

[44] Catalogna G, Talarico C, Dattilo V, Gangemi V, Calabria F, and D'Antona L, et al (2017). The SGK1 kinase inhibitor SI113 sensitizes theranostic effects of the 64CuCl2 in human glioblastoma multiforme cells. *Cell Physiol Biochem* **43**, 108–119.

[45] Abbruzzese C, Catalogna G, Gallo E, di Martino S, Mileo AM, and Carosi M, et al (2017). The small molecule SI113 synergizes with mitotic spindle poisons in arresting the growth of human glioblastoma multiforme. *Oncotarget* **8**, 110743–110755.

[46] Rensen WM, Roscioli E, Tedeschi A, Mangiacasale R, Ciciarello M, and Di Gioia SA, et al (2009). RanBP1 downregulation sensitizes cancer cells to taxol in a caspase-3–dependent manner. *Oncogene* **28**, 1748–1758.

[47] D'Antona L, Amato R, Talarico C, Ortuso F, Menniti M, and Dattilo V, et al (2015). SI113, a specific inhibitor of the Sgk1 kinase activity that counteracts cancer cell proliferation. *Cell Physiol Biochem* **35**. http://dx.doi.org/10.1159/000374008.

[48] Ferlini C, Raspaglio G, Mozzetti S, Distefano M, Filippetti F, and Martinelli E, et al (2003). Bcl-2 down-regulation is a novel mechanism of paclitaxel resistance. *Mol Pharmacol* **64**, 51–58.

[49] Concolino A, Olivo E, Tammè L, Fiumara CV, De Angelis MT, and Quaresima B, et al (2018). Proteomics analysis to assess the role of mitochondria in BRCA1-mediated breast tumorigenesis. *Proteomes* **6**, 16.

[50] Qu Y, Cong P, Lin C, Deng Y, Li-Ling J, and Zhang M (2017). Inhibition of paclitaxel resistance and apoptosis induction by cucurbitacin B in ovarian carcinoma cells. *Oncol Lett* **14**, 145–152.

[51] Ortuso F, Amato R, Artese A, D'antona L, Costa G, and Talarico C, et al (2014). In silico identification and biological evaluation of novel selective serum/glucocorticoid-inducible kinase 1 inhibitors based on the pyrazolo-pyrimidine scaffold. *J Chem Inf Model* **54**, 1828–1832.

[52] Ma X, Zhang L, Song J, Nguyen E, Lee RS, and Rodgers SJ, et al (2019). Characterization of the Src-regulated kinome identifies SGK1 as a key mediator of Src-induced transformation. *Nat Commun* **10**, 296.

[53] Wittmann-Liebold B, Graack H-R, and Pohl T (2006). Two-dimensional gel electrophoresis as tool for proteomics studies in combination with protein identification by mass spectrometry. *Proteomics* **6**, 4688–4703.

[54] Rabilloud T and Lelong C (2011). Two-dimensional gel electrophoresis in proteomics: a tutorial. *J Proteome* **74**, 1829–1841.

[55] Scumaci D, Tammè L, Fiumara CV, Pappaianni G, Concolino A, and Leone E, et al (2015). Plasma proteomic profiling in hereditary breast cancer reveals a BRCA1-specific signature: diagnostic and functional implications. *PLoS One* **10**e0129762.

[56] Shevchenko A, Wilm M, Vorm O, and Mann M (1996). Mass spectrometric sequencing of proteins silver-stained polyacrylamide gels. *Anal Chem* **68**, 850–858.

[57] Stensballe A and Jensen ON (2001). Simplified sample preparation method for protein identification by matrix-assisted laser desorption/ionization mass spectrometry: in-gel digestion on the probe surface. *Proteomics* **1**, 955–966.

[58] Fiumara CV, Scumaci D, Iervolino A, Perri AM, Concolino A, and Tammè L, et al (2018). Unraveling the mechanistic complexity of the glomerulocystic phenotype in dicer conditional KO mice by 2D gel electrophoresis coupled mass spectrometry. *Proteomics Clin Appl* **12**e1700006.

[59] Vandesompele J, De Preter K, Pattyn F, Poppe B, Van Roy N, and De Paepe A, et al (2002). Accurate normalization of real-time quantitative RT-PCR data by geometric averaging of multiple internal control genes. *Genome Biol* **3** RESEARCH0034.